Possible Frustration Effects on a New Antiferromagnetic Compound Ce6Pd13Zn4 with the Octahedral Ce Sublattice

Matsuoka, Eiichi
Oshima, Akihiro
Sugawara, Hitoshi
Sakurai, Takahiro
Ohta, Hitoshi

(Citation)
Journal of the Physical Society of Japan,87(1):013705-013705

(Issue Date)
2018-01-15

(Resource Type)
journal article

(Version)
Accepted Manuscript

(URL)
https://hdl.handle.net/20.500.14094/90004871

Possible Frustration Effects on a New Antiferromagnetic Compound $Ce_6Pd_{13}Zn_4$ with the Octahedral Ce Sublattice

Eiichi Matsuoka[1*], Akihiro Oshima[1], Hitoshi Sugawara[1], Takahiro Sakurai[2], and Hitoshi Ohta[3]

[1]*Department of Physics, Graduate School of Science, Kobe University, Kobe 657-8501, Japan*
[2]*Research Facility Center for Science and Technology, Kobe University, Kobe 657-8501, Japan*
[3]*Molecular Photoscience Research Center, Kobe University, Kobe 657-8501, Japan*

(Received October 2, 2017)

Magnetization, specific heat, and electrical resistivity measurements have been performed on polycrystalline samples of a new cubic compound, $Ce_6Pd_{13}Zn_4$. This compound exhibits metallic behavior and is classified as a Kondo-lattice system. The trivalent Ce ions are responsible for the antiferromagnetic transition at T_N = 3.3 K and the phase transition at T_N' = 1.3 K with the formation of superzone gaps. The increase in magnetic susceptibilities below T_N and the considerably large value of the specific heat divided by temperature (1.25 $J \cdot Ce\text{-}mol^{-1} \cdot K^{-2}$) imply the existence of non-ordered Ce magnetic moments due to the geometrical frustration on the octahedral Ce sublattice.

Geometrical frustration hinders a simple collinear antiferromagnetic (AFM) order and causes a variety of attractive magnetic phenomena. For insulators, the spin-ice state of the pyrochlore compounds[1)] and the quantum spin-liquid state of compounds with triangular and Kagomé lattices[2)] are the distinctive examples of such phenomena. The metallic rare-earth and actinide compounds are marked compounds from the standpoint of frustration: if the rare-earth or actinide ions are located on the geometrically frustrated sites, the effects of frustration as well as the strong correlation effects between *f* and the conduction electrons offer novel magnetic and transport properties. The peculiar AFM structures in CePdAl[3)] and UNi_4B[4)] that are characterized by the existence of non-ordered magnetic moments, the extremely small release of magnetic entropy at the magnetic transition temperature in YbAgGe[5)], and the quantum critical behavior in Ce_2Pt_2Pb[6)] are examples of frustration-driven phenomena for metallic *f*-electron compounds. To explore novel phenomena related to the strong correlation and frustration effects, it is important to search for new compounds and study their physical properties. In the present letter, we report on the magnetic and transport properties of a new cubic compound, $Ce_6Pd_{13}Zn_4$. The existence of this compound was

reported recently by Gerke *et al.*[7] Figure 1 shows the chemical unit cell of $Ce_6Pd_{13}Zn_4$. This cell can be considered as the body-centered-cubic arrangement of the Pd1-centered Ce_6 octahedra surrounded by a $[Pd_{12}Zn_4]$ network.[7] The site symmetry of the Ce ions (12*e* Wyckoff site) is not cubic but tetragonal in this structure. The first and the second nearest Ce ions are connected by the red and blue lines, respectively. If the second nearest Ce ions, which form the edges of the octahedra, interact antiferromagnetically, frustration of the Ce magnetic moments hinders a collinear AFM arrangement to be formed. Therefore, $Ce_6Pd_{13}Zn_4$ can be considered as a rare candidate of the three-dimensional frustration system. We examined the physical properties of $Ce_6Pd_{13}Zn_4$ for the first time and found that this compound exhibits a rather unusual AFM order where non-ordered Ce magnetic moments seem to exist due to the frustration.

In Ref. 7, polycrystalline samples of $RE_6Pd_{13}Zn_4$ (*RE* = La-Nd, Sm, Gd, Tb) were grown by melting the constituent elements in niobium tubes. Instead of using a niobium tube, we grew the polycrystalline samples by arc melting and subsequent heat treatment. First, the intermediate alloy Ce_6Pd_{13} was synthesized by arc melting the 6:13 mixture of Ce (99.9%) and Pd (99.99%) in an Ar gas atmosphere. Powdered Ce_6Pd_{13} and Zn (99.9999%) with the molar ratio 1:4 were then melted in the BN (boron nitride) crucible sealed in the evacuated quartz tube. The quartz tube was heated rapidly (400 K/hour) up to 670 K in the muffle furnace, then heated slowly (60 K/hour) to 1170 K and kept at this temperature for 12 hours to ensure a homogeneous mixture of the elements. To grow a sample of the nonmagnetic reference compound $La_6Pd_{13}Zn_4$, $La_{4.5}Pd_{13}$ was synthesized first by arc melting the 4.5:13 mixture of La and Pd. Powdered $La_{4.5}Pd_{13}$, La, and Zn with the molar ratio 1:1.5:4 were then melted in the BN crucible sealed in the evacuated quartz tube. These samples were characterized by X-ray powder diffraction experiments using a diffractometer with Cu-$K_{\alpha 1}$ radiation (Rigaku, MiniFlexII). Almost all the Bragg peaks appearing in the diffraction patterns can be indexed on the basis of a site occupancy variant of the $Dy_6Fe_{16}O$-type structure (space group $Im\bar{3}m$, O_h^9, No. 229), although small peaks of unidentified impurity phases are discernible for $Ce_6Pd_{13}Zn_4$. No distinctive impurity peaks are observed in the pattern of $La_6Pd_{13}Zn_4$. The lattice constants determined by X-ray diffraction experiments at room temperature are a = 9.621(1) Å for $Ce_6Pd_{13}Zn_4$ and a = 9.683(1) Å for $La_6Pd_{13}Zn_4$. The a value of the Ce compound agrees with that reported previously, whereas the a value of the La compound agrees with that of the non-stoichiometric compound $La_6Pd_{13-x}Zn_{4+x}$.[7] The magnetic, thermal, and transport properties of these samples were examined by magnetization, $M(T, H)$, specific heat, $C(T)$, and electrical resistivity, $\rho(T, H)$, measurements as functions of

the temperature T and magnetic field H. $M(T, H)$ was measured using a superconducting quantum interference device magnetometer (Quantum Design, MPMS) between 1.8 and 300 K up to 5 T. $C(T)$ was measured with a thermal relaxation method between 0.6 and 9 K in a laboratory-built ^{3}He cryostat. $\rho(T, H)$ was measured with a dc four-probe method between 0.4 and 294 K up to 9 T in a laboratory-built ^{3}He cryostat.

Figure 2(a) shows the temperature dependence of the inverse magnetic susceptibility, H/M, of $Ce_6Pd_{13}Zn_4$. The H/M above 100 K can be fitted using the formula $H/M = 1/[C_{Curie}/(T - \theta_P) + \chi_0]$, where $C_{Curie} = 0.832$ emu·K/Ce-mol, $\theta_P = -13$ K, and $\chi_0 = -3.45\times10^{-4}$ emu/Ce-mol represent a Curie constant, the paramagnetic Curie temperature, and the sum of the contributions of the core diamagnetism and Pauli paramagnetism, respectively. The solid line in Fig. 2(a) is a result of using this formula. The χ_0 obtained from this fitting is comparable to the M/H at 300 K for $La_6Pd_{13}Zn_4$ (-1.61×10^{-4} emu/La-mol). The effective magnetic moment μ_{eff} calculated from C_{Curie} is 2.58 μ_B/Ce, implying that the Ce ions in this compound are trivalent because μ_{eff} is very close to that of the free Ce^{3+} ion (2.54 μ_B/Ce).

Figure 2(b) shows the temperature dependences of the magnetic susceptibilities, M/H's, of $Ce_6Pd_{13}Zn_4$. The M/H measured at 0.1 T shown as black circles exhibits an inflection at T_N = 3.3 K (see the arrow in the Fig. 2(b)). Here, T_N is defined as the minimum temperature of $d^2(M/H)/dT^2$. T_N decreases with increasing magnetic field, and no anomalies are observed in the M/H at 5 T. The M/H at 0.1 T has a broad maximum and a minimum at 3 K and 2.5 K, respectively, before showing a gradual increase below 2.5 K, while that at $\mu_0H \geq 1$ T increases continuously below T_N with no maximum or minimum. The decrease in T_N by magnetic fields suggests that the AFM transition occurs at T_N, although the increase in M/H below T_N is not typical for antiferromagnets. One possible explanation for the increase in M/H is that the Curie–Weiss tail of the impurity phases is observed in M/H. To evaluate the impurity effects, we grew the other sample of $Ce_6Pd_{13}Zn_4$ in the same way we grew $La_6Pd_{13}Zn_4$; i.e., $Ce_{4.5}Pd_{13}$ was used as an intermediate alloy. No impurity peaks were observed in the X-ray diffraction pattern of this sample, and the lattice constant (a = 9.618(2) Å) agrees with that of the non-stoichiometric compound $Ce_6Pd_{13-x}Zn_{4+x}$.[7] The M/H of this purer sample also shows an increase in M/H below T_N as shown by the red down-pointing triangles in Fig. 2(b), suggesting that the impurity phases are unlikely to increase the M/H. Therefore, we have to consider the increase in M/H to be intrinsic and inherent in the AFM phase.

The magnetic-field dependences of the magnetization M are shown in Fig. 3(a). In contrast to the paramagnetic field dependence of M at 5 K ($> T_N$), M at 1.8 K ($< T_N$) shows

two anomalies at μ_0H_1 = 0.3 T and μ_0H_2 = 3.5 T. Here, μ_0H_1 and μ_0H_2 were defined as the maximum field and the inflection point of dM/dH, respectively, as shown by the arrows in Fig. 3(b). The anomaly at μ_0H_1 is metamagnetic, as shown by the arrow in the inset, while that at μ_0H_2 corresponds to the broad shoulder of M. The appearance of the two anomalies implies that the magnetic structure below μ_0H_1 is different from that at $\mu_0H_1 < \mu_0H < \mu_0H_2$. No spontaneous or remanent moment at 1.8 K suggests the occurrence of the AFM transition at T_N. The anomalies corresponding to the μ_0H_1 and μ_0H_2 appear in the magnetic-field dependences of the electrical resistivity, as described later.

Figure 4(a) shows the temperature dependences of the specific heats C of $Ce_6Pd_{13}Zn_4$ and $La_6Pd_{13}Zn_4$. The $C(T)$ of $Ce_6Pd_{13}Zn_4$ exhibits a gradual increase with decreasing temperature, followed by a steep increase below 3.5 K, and shows an anomaly peaked at 3.1 K. The appearance of the $C(T)$ anomaly suggests that the inflection of M/H at T_N is due to the second-order AFM transition. The gradual increase of $C(T)$ between 9 and 3.5 K might reflect a development in the short-range magnetic correlation. At T_N' =1.3 K, $C(T)$ has a shoulder as shown by the dotted arrow in Fig. 4(a), which corresponds to a resistivity anomaly mentioned later. The temperature dependence of the magnetic entropy S_{mag} was calculated by integrating C_{mag}/T in T, where C_{mag} is the magnetic specific heat that was deduced by subtracting the $C(T)$ of $La_6Pd_{13}Zn_4$ from that of $Ce_6Pd_{13}Zn_4$. Because the $C(T)$ measurement of $La_6Pd_{13}Zn_4$ was limited to 1.7 K, the $C(T)$ of $La_6Pd_{13}Zn_4$ below 1.7 K was calculated using the fitted result of the C/T versus T^2 plot by the formula $C/T = \gamma + \beta T^2$, where γ= 0.0042 J·La-mol^{-1}·K^{-2} and β = 4.4 × 10^{-4} J·La-mol^{-1}·K^{-4} represent the electronic and phonon specific heat coefficients, respectively. As shown in Fig. 4(a), S_{mag} shows an inflection at T_N = 3.3 K. The sixfold ground multiplet of Ce^{3+} splits into three doublets because the site symmetry of the Ce ions is tetragonal, as mentioned above. Because S_{mag} at T_N (3.9 J·mol^{-1}·K^{-1}) is 68% of Rln2 (R: gas constant), we can consider the ground doublet of Ce^{3+} to be responsible for the AFM transition at T_N. The 32% reduction of S_{mag} from Rln2 can be ascribed to the Kondo effect and the entropy release above T_N due to the short-range magnetic correlation. The S_{mag} reduction might be related to the considerably large C/T below T_N. The C/T value at T_N' is 1.25 J·Ce-mol^{-1}·K^{-2}, which is comparable to the electronic specific heat coefficient of heavy-fermion compounds such as $CeCu_2Si_2$.[8] Below T_N', C/T decreases steeply with decreasing temperature and reduces to 0.47 J·Ce-mol^{-1}·K^{-2} at 0.6 K. To estimate the Kondo temperature T_K of $Ce_6Pd_{13}Zn_4$, we referred to a numerical calculation of the relationship between T/T_K and the S_{mag} based on a spin 1/2 Kondo model.[9] T_K was estimated to be 2.9 K

by comparing the experimental S_{mag} at T_N with this calculation.

Figure 5(a) shows the temperature dependence of the electrical resistivity ρ of $Ce_6Pd_{13}Zn_4$. $\rho(T)$ decreases with decreasing temperature down to 10 K as shown in the inset of Fig. 5(a), which is followed by a minimum at 10 K as shown in the main panel. The appearance of the $\rho(T)$ minimum at 10 K suggests that $Ce_6Pd_{13}Zn_4$ can be classified as a Kondo-lattice system. Below the minimum temperatures of 3.6 K and 1.25 K that correspond to T_N and T_N', $\rho(T)$ increases with decreasing temperature before showing maximums at 3.1 K and 1.1 K, respectively. Two causes can be considered for the $\rho(T)$ increase below the magnetic transition temperature: one is the spin density wave transition due to the conduction electrons, and the other is the formation of a superzone gap accompanied by the AFM transition of the localized moments. Because the AFM transition at T_N can be ascribed to the localized 4*f* electrons as revealed by the $C(T)$ measurement, we can consider the $\rho(T)$ increase below T_N to result from the formation of a superzone gap. If this is the case, the $\rho(T)$ increase below T_N' might reflect the reconstruction of the superzone gap that is concomitant with a change in the magnetic structure. Figure 5(b) represents the magnetic-field dependences of ρ measured by applying a magnetic field parallel to the current *I*. At 4.2 K ($> T_N$), $\rho(H)$ decreases monotonously with increasing magnetic field up to 9 T, which is ascribed to the suppression of the Kondo effect. $\rho(H)$ at 1.5 K ($< T_N$) and 0.44 K ($< T_N'$) decrease more steeply by application of a magnetic field and show two anomalies at approximately 0.3 and 4 T. These magnetic fields coincide approximately with the $\mu_0 H_1$ and $\mu_0 H_2$ determined by the magnetization measurements. Above 4 T, $\rho(H)$ at 1.5 and 0.44 K are weakly field dependent. Such $\rho(H)$ behaviors at 1.5 and 0.44 K suggest that the superzone gap is gradually narrowed by application of a magnetic field and closed above 4 T. In fact, similar $\rho(H)$ behavior was reported for $CeSbNi_{0.15}$ where the AFM superzone gap is constructed.[10)]

The decrease in T_N obtained by applying a magnetic field and the absence of a spontaneous or remanent moment below T_N strongly support the AFM nature of the ordered state of $Ce_6Pd_{13}Zn_4$. In contrast, the increase in M/H below T_N is not typical for antiferromagnets. To understand the causes of these contrasting behaviors, we have to estimate the AFM structure below T_N. Because of the octahedral arrangement of the Ce ions, the AFM structure must have the character to compromise with the frustration effect. In this situation, it is instructive to refer to the AFM structures of the cubic Cu_3Au-type compound Mn_3Pt, whose Mn ions form octahedra. Mn_3Pt shows a paramagnetic-AFM transition at 475 K and an AFM-AFM one at 365 K.[11)] In the high-temperature AFM phase (F-phase), one third

of the Mn moments take a non-ordered or nonmagnetic state, and the remaining two thirds of the moments participate in the collinear AFM order.[11–13] On the other hand, all of the Mn moments, which lie on the (111) plane and point to the [211] direction, participate in the non-collinear AFM order in the low-temperature AFM phase (D-phase).[11–13] If the magnetic structure of $Ce_6Pd_{13}Zn_4$ below T_N is similar to that of the D-phase, M/H must decrease below T_N because no paramagnetic Ce moments exist in such a state. We therefore consider the AFM structure below T_N to be similar to that of the F-phase; i.e., non-ordered Ce magnetic moments exist. In the case of rare-earth compounds, the existence of non-ordered magnetic moments due to frustration was suggested for $SmPt_2Si_2$[14] and $Ce_5Ni_2Si_3$[15] by the increase in M/H below T_N. The large electronic specific heat coefficient of $SmPt_2Si_2$ (350 $mJ \cdot mol^{-1} \cdot K^{-2}$) was also ascribed to the frustration: non-ordered Sm ions form a Kondo sublattice through hybridization with conduction electrons, resulting in quasiparticle mass enhancement.[14] If the non-ordered Ce moments exist in $Ce_6Pd_{13}Zn_4$, the considerably large C/T value at T_N' (1.25 $J \cdot Ce\text{-}mol^{-1} \cdot K^{-2}$) can be explained by the similar mechanism for $SmPt_2Si_2$. The steep decrease in C/T below T_N' might reflect the appearance of the D-phase-like state, where all of the Ce moments contribute.

In summary, the physical property measurements of a new cubic compound $Ce_6Pd_{13}Zn_4$ revealed that this compound exhibits metallic behavior and is classified as a Kondo-lattice system. The trivalent Ce ions are responsible for the antiferromagnetic transition at $T_N = 3.3$ K and the phase transition at $T_N' = 1.3$ K with the formation of superzone gaps. The increase in the magnetic susceptibility below T_N and the considerably large value of the specific heat divided by the temperature imply the existence of non-ordered Ce magnetic moments due to the geometrical frustration on the octahedral Ce sublattice. We therefore conclude that $Ce_6Pd_{13}Zn_4$ is one of the rare metallic compounds with the three-dimensional frustration. To confirm the effects of the frustration microscopically, the determination of magnetic structures by neutron diffraction experiments is indispensable. For this purpose, growth of single-crystalline samples of $Ce_6Pd_{13}Zn_4$ is now under way.

Acknowledgments

We thank Professor Kenji Ohoyama of the Graduate School of Science and Engineering, Ibaraki University, for the valuable discussions about the magnetic structures of $Ce_6Pd_{13}Zn_4$. We are indebted to Professors Kazushige Tomeoka and Yusuke Seto of the Department of Planetology, Kobe University, for assisting with the electron-probe microanalysis and for the fruitful discussions about the data analyses.

*E-mail: matsuoka@crystal.kobe-u.ac.jp

1) S. T. Bramwell and M. J. P. Gingras, Science **294**, 1495 (2001)
2) L. Balents, Nature **464**, 199 (2010).
3) A. Dönni, G. Ehlers, H. Maletta, P. Fischer, H. Kitazawa, and M. Zolliker, J. Phys.: Condens. Matter **8**, 11213 (1996).
4) S. A. M. Mentink, A. Drost, G. J. Nieuwenhuys, E. Frikkee, A. A. Menovsky, and J. A. Mydosh, Phys. Rev. Lett. **73**, 1031 (1994).
5) K. Umeo, K. Yamane, Y. Muro, K. Katoh, Y, Niide, A. Ochiai, T. Morie, T. Sakakibara, and T. Takabatake, J. Phys. Soc. Jpn. **73**, 537 (2004).
6) M. S. Kim and M. C. Aronson, J. Phys.: Condens. Matter **23**, 164204 (2011).
7) B. Gerke, O. Janka, and R. Pöttgen, Z. Anorg. Allg. Chem. **640**, 2747 (2014).
8) F. Steglich, J. Aarts, C. D. Bredl, W. Lieke, D. Meschede, W. Franz, and H. Schäfer, Phys. Rev. Lett. **43**, 1892 (1979).
9) H. -U. Desgranges and K. D. Schotte, Phys. Lett. **91A**, 240 (1982).
10) M. H. Jung, D. T. Adroja, N. Kikugawa, T. Takabatake, I. Oguro, S. Kawasaki, and K. Kindo, Phys. Rev. B **62**, 13860 (2000).
11) T. Ikeda and Y. Tsunoda, J. Phys. Soc. Jpn. **72**, 2614 (2003).
12) E. Krén, G. Kádár, L. Pál, J. Sólyom, P. Szabó, and T. Tarnóczi, Phys. Rev. **171**, 574 (1968).
13) K. Tomiyasu, H. Yasui, and Y. Yamaguchi, J. Phys. Soc. Jpn. **81**, 114724 (2012).
14) K. Fushiya, T. D. Matsuda, R. Higashinaka, K. Akiyama, and Y. Aoki, J. Phys. Soc. Jpn. **83**, 113708 (2014).
15) B. K. Lee, D. H. Ryu, D. Y. Kim, J. B. Hong, M. H. Jung, H. Kitazawa, O. Suzuki, S. Kimura, and Y. S. Kwon, Phys. Rev. B **70**, 224409 (2004).

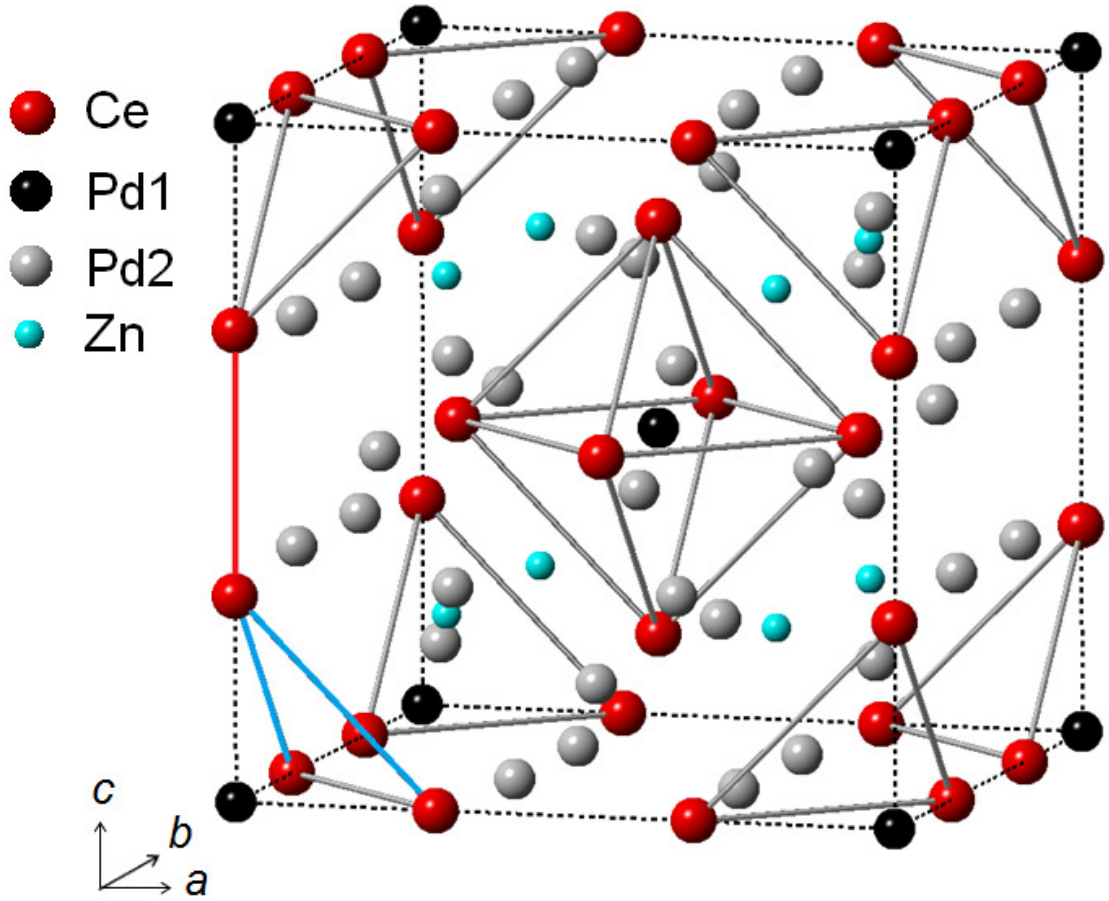

Fig. 1. (Color online) The chemical unit cell of $Ce_6Pd_{13}Zn_4$. The Pd1-centered Ce_6 octahedra are emphasized. The first and the second nearest Ce ions are connected by the red and blue lines, respectively.

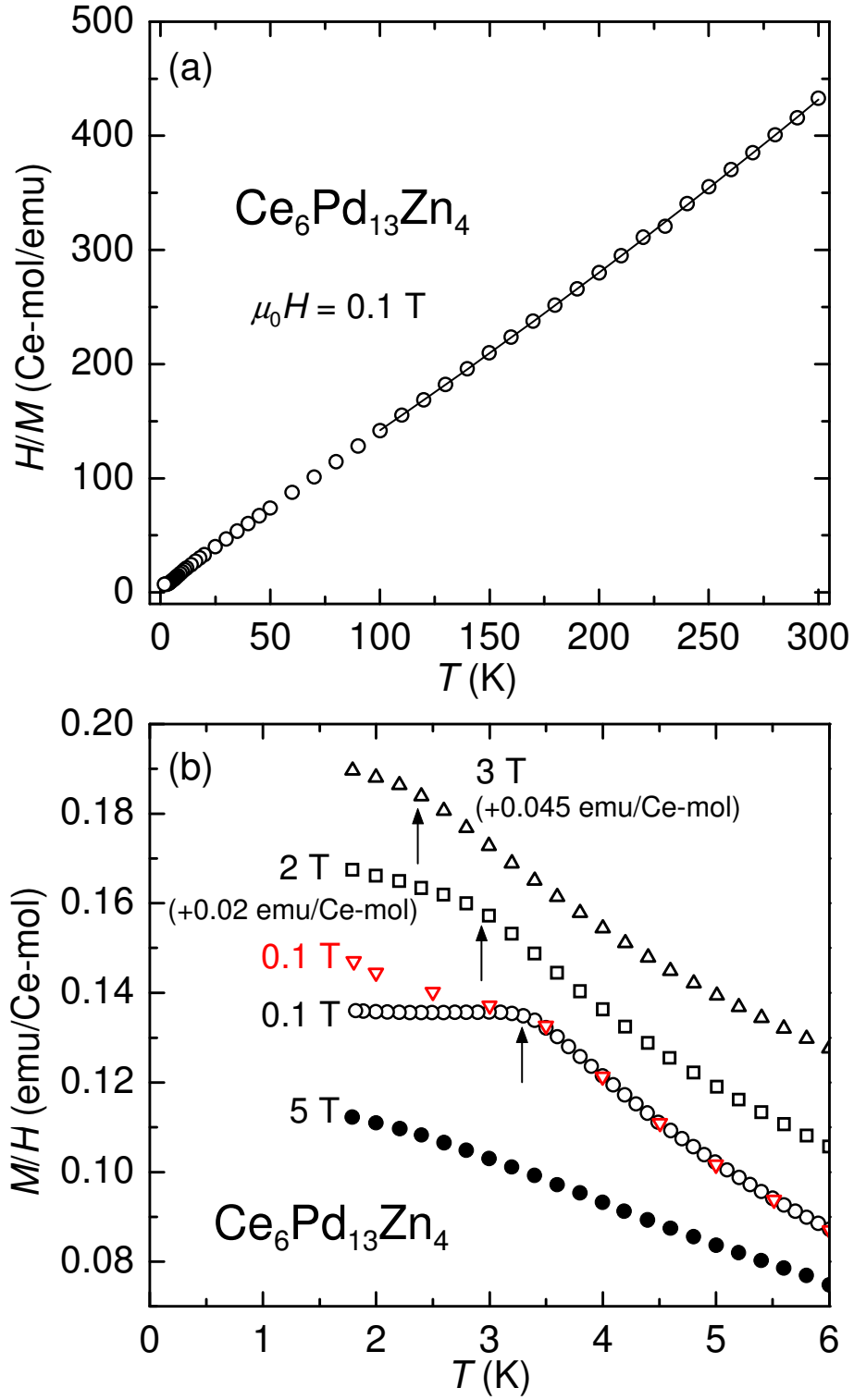

Fig. 2. (Color online) (a) Temperature-dependent inverse magnetic susceptibility H/M and (b) magnetic susceptibility M/H of $Ce_6Pd_{13}Zn_4$. The red down-pointing triangles in (b) represent M/H of the purer sample (see text). The arrows in (b) show T_N. The M/H values measured at 2 and 3 T are shifted vertically by the values in parentheses for ease of observation.

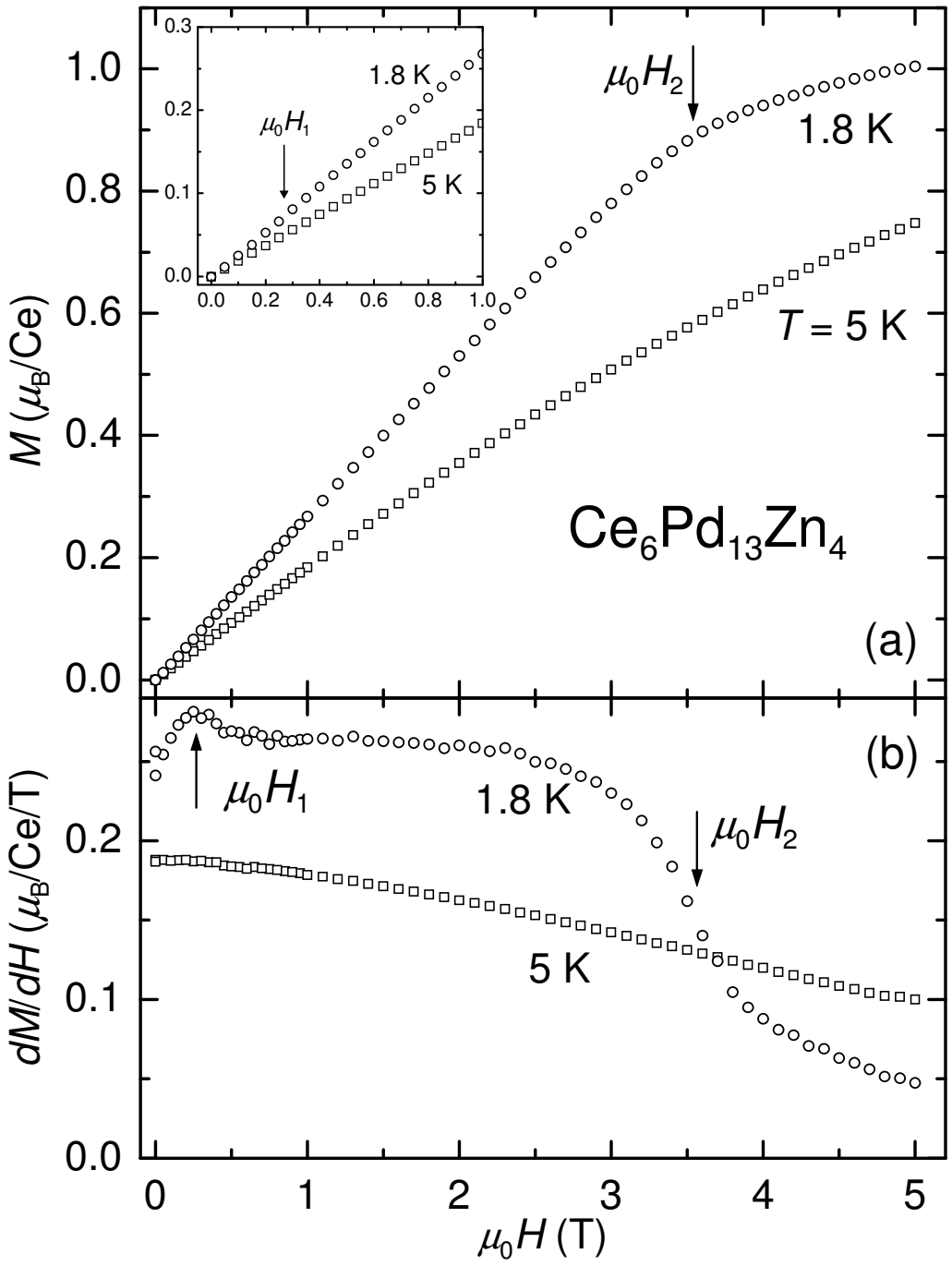

Fig. 3. (a) The isothermal magnetization $M(H)$ and (b) dM/dH of $Ce_6Pd_{13}Zn_4$. The inset in (a) represents the low-field region of $M(H)$.

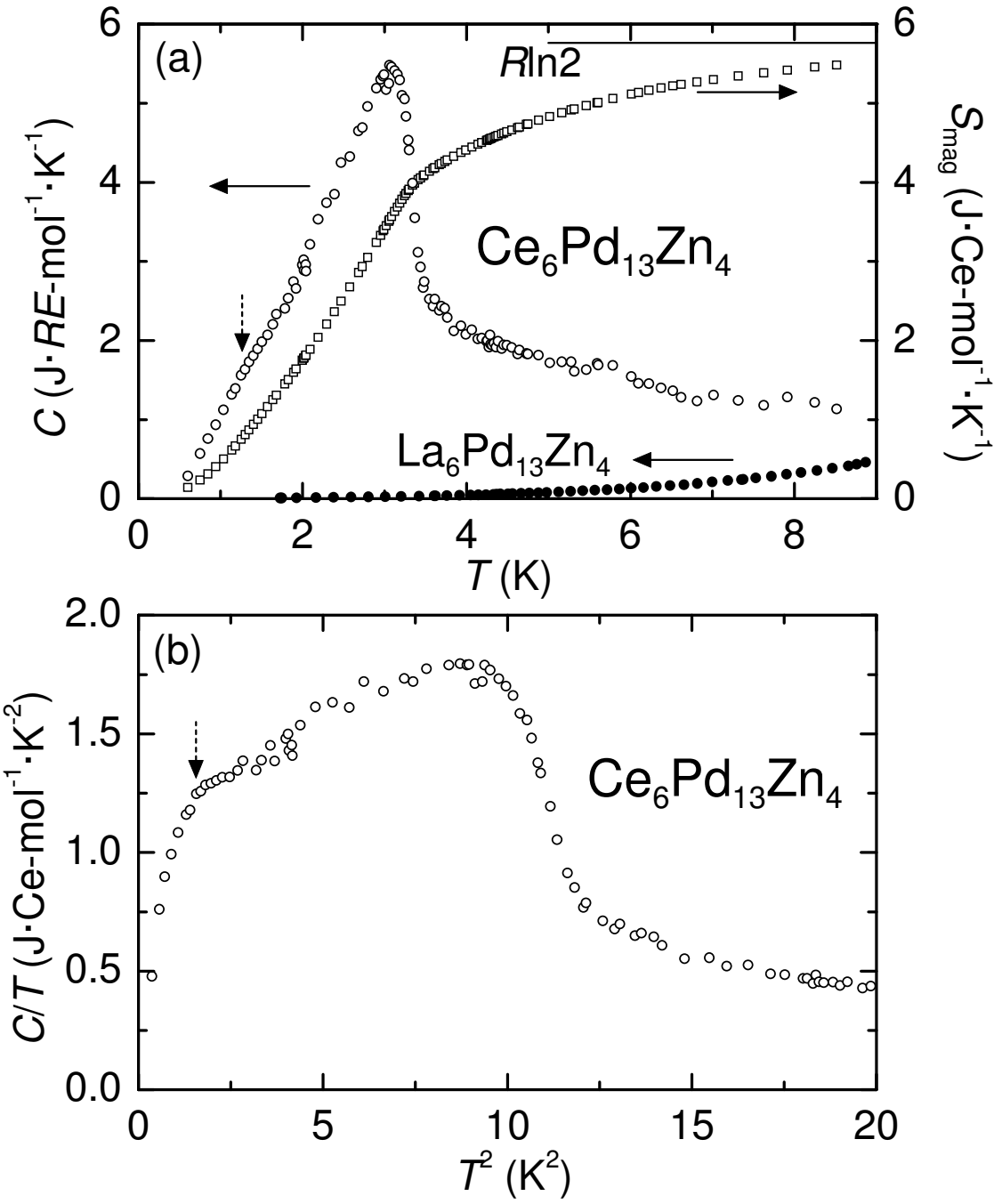

Fig. 4. (a) Temperature dependences of specific heat C and magnetic entropy S_{mag} of $Ce_6Pd_{13}Zn_4$ (open symbols). The C of $La_6Pd_{13}Zn_4$ (solid circles) is shown for comparison. (b) C/T vs. T^2 of $Ce_6Pd_{13}Zn_4$. The dotted arrows in (a) and (b) represent the transition temperature T_N'.

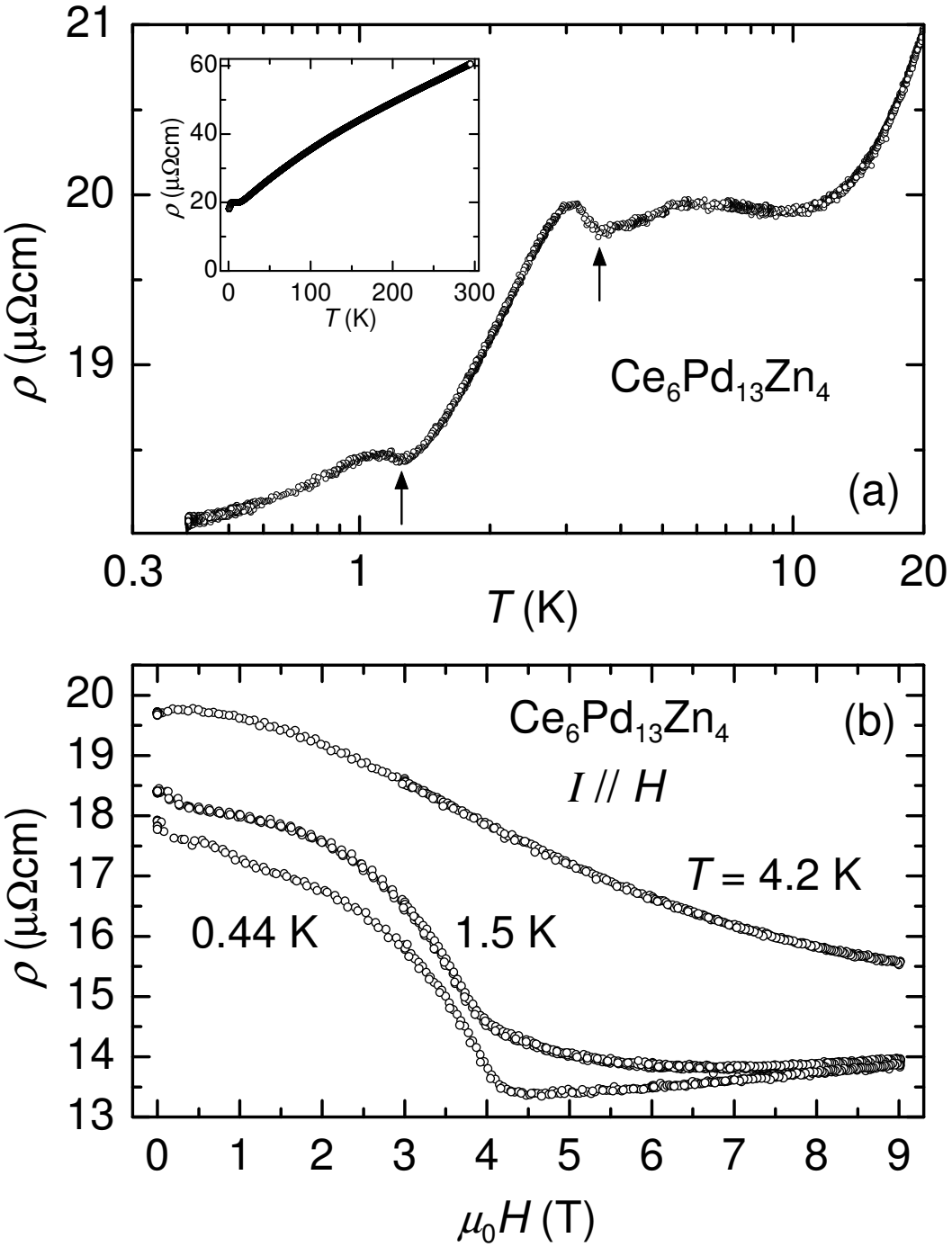

Fig. 5. (a) Temperature dependence of the electrical resistivity ρ of $Ce_6Pd_{13}Zn_4$ below 20 K. The arrows show minimum temperatures of ρ corresponding to T_N and T_N'. The inset shows the ρ up to 294 K. (b) Magnetic-field dependences of ρ of $Ce_6Pd_{13}Zn_4$ at various temperatures.